Inorg. Chem. **2007**, *46*, 7601–7609

Ionic and Neutral C_{60} Complexes with Coordination Assemblies of Metal Tetraphenylporphyrins, $M^{II}TPP_2$·DMP (M = Mn, Zn). Coexistence of $(C_{60}^-)_2$ Dimers Bonded by One and Two Single Bonds in the Same Compound

Dmitri V. Konarev,*,†,‡ Salavat S. Khasanov,†,§ Gunzi Saito,*,† Akihiro Otsuka,|| and Rimma N. Lyubovskaya‡

Division of Chemistry, Graduate School of Science, Kyoto University, Sakyo-ku, Kyoto 606-8502, Japan, Institute of Problems of Chemical Physics RAS, Chernogolovka, Moscow region 142432, Russia, Institute of Solid State Physics RAS, Chernogolovka, Moscow region 142432, Russia, and Research Center for Low Temperature and Materials Sciences, Kyoto University, Sakyo-ku, Kyoto 606-8502, Japan

Received August 29, 2006

Coordination assemblies of metal tetraphenylporphyrins, $M^{II}TPP_2$·DMP (M = Mn, Zn) were shown to form ionic multicomponent and neutral complexes with fullerene, $\{(Mn^{II}TPP)_2$·DMP$\}$·$(C_{60}^-)_2$·$(DMETEP^+)_2$·$(C_6H_4Cl_2)_5$ (**1**) and $\{(ZnTPP)_2$·DMP$\}$·$(C_{60})_2$·$(C_6H_5Cl)_4$ (**2**), where DMP = *N,N*′-dimethylpiperazine and $DMETEP^+$ = the cation of *N,N*′-dimethyl-*N*′-ethylthioethylpiperazine. The crystal structure of **1** contains zigzag chains of the $(C_{60}^-)_2$ dimers alternating with the $DMETEP^+$ cations in the channels formed by the $(Mn^{II}TPP)_2$·DMP units, whereas in **2** zigzag chains of the C_{60} molecules are separated by the $(ZnTPP)_2$·DMP units and C_6H_5Cl molecules. The $(M^{II}TPP)_2$·DMP assemblies (M = Mn, Zn) have axial M–N(DMP) bonds of 2.315(2) and 2.250(2) Å length, average equatorial M–N(DMP) bonds elongated to 2.141(3) and 2.077(2) Å, and M^{II} atoms displaced from the porphyrin plane toward the ligand by 0.677 and 0.485 Å, respectively. The single-bonded σ-$(C_{60}^-)_2$ dimer coexists in **1** with the $(C_{60}^-)_2$ dimer bonded by two single bonds with 86/14 occupancy factors. The σ-$(C_{60}^-)_2$ dimers are unusually stable and begin to dissociate only above a temperature of 320–330 K that results in the increase of the magnetic moment of **1** from 8.33 μ_B (320 K) to 8.66 μ_B (360 K). The electron paramagnetic resonance (EPR) signal of the dimeric phase (T < 320 K) with the features spread over the range of 0–0.7 T was attributed to the interacting Mn^{2+} centers in the $(Mn^{II}TPP)_2$·DMP units. The dissociation of the σ-$(C_{60}^-)_2$ dimers to the EPR-active $C_{60}^{\bullet-}$ radical anions manifests a new broad Lorenz signal above 320 K with g = 2.0179 and ΔH = 65.5 mT. This signal can appear due to the exchange coupling between paramagnetic $(Mn^{II}TPP)_2$·DMP and $C_{60}^{\bullet-}$ species. The vis–NIR spectrum of the σ-$(C_{60}^-)_2$ dimers is discussed.

Introduction

Ionic fullerene compounds are interesting by their physical properties[1] and a large variety of dimeric and polymeric structures of negatively charged fullerenes, some of which show metallic conductivity and strong antiferromagnetic interactions.[2] The dimerization of fullerene radical anions reversibly affects the magnetic properties of the complexes and is accompanied by paramagnetic−diamagnetic transitions or the decrease of the magnetic moment of the complexes.[3] Now, dimerization has been found in several ionic complexes and salts of C_{60}. Those are metastable M·C_{60} phases (M =

* To whom correspondence should be addressed. E-mail: konarev@icp.ac.ru (D.V.K), saito@kuchem.kyoto-u.ac.jp (G.S.). Fax: +007-496-522-18-52 (D.V.K.), +81-75-753-40-35 (G.S.).
† Division of Chemistry, Graduate School of Science, Kyoto University.
‡ Institute of Problems of Chemical Physics RAS.
§ Institute of Solid State Physics RAS.
|| Research Center for Low Temperature and Materials Sciences, Kyoto University.

(1) (a) Rosseinsky, M. J. *J. Mater. Chem.* **1995**, *5*, 1497. (b) Gotschy, B. *Fullerene Sci. Technol*. **1996**, *4*, 677. (c) Konarev, D. V.; Lyubovskaya, R. N. *Russ. Chem. Rev*. **1999**, *68*, 19.
(2) Prassides, K. *The Physics of Fullerenes-Based and Fullerene-Related Materials*; W. Andreoni, Ed.; Kluwer Academic Publishers: The Netherlands, 2000; p 175.

10.1021/ic061628z CCC: $37.00
Published on Web 08/08/2007

K, Rb, Cs);[4] $Cr(C_6H_5Me)_2{\cdot}C_{60}$ ($Cr(C_6H_5Me)_2$ = bis(toluene)-chromium) at 250 K;[5] $Cp^*_2Cr{\cdot}C_{60}{\cdot}(C_6H_4Cl_2)_2$ (Cp^*_2Cr = decamethylchromocene) at 220−200 K;[6] $Cr(C_6H_6)_2{\cdot}C_{60}{\cdot}C_6H_4Cl_2$ and $Cr(C_6H_6)_2{\cdot}C_{60}{\cdot}C_6H_5CN$ ($Cr(C_6H_6)_2$ = bis-(benzene)chromium) at 160−240 and above 250 K, respectively;[6b,7] $Cp_2Co{\cdot}C_{60}{\cdot}C_6H_4Cl_2$ (Cp_2Co = cobaltocene) at 250−350 K;[6b] $Cr(C_6H_5-C_6H_5)_2{\cdot}C_{60}$ ($Cr(C_6H_5-C_6H_5)_2$ = bis(diphenyl)-chromium);[8] multicomponent $(Cs)_2{\cdot}(C_{60})_2{\cdot}CTV{\cdot}(DMF)_6$ (CTV = cyclotriveratrylene) at 140−220 K;[3] and $Cr(C_6H_6)_2{\cdot}C_{60}{\cdot}[Pd(dbdtc)_2]_{0.5}$ ($Pd(dbdtc)_2$ = palladium(II) dibenzyldithiocarbamate) at 130−150 K.[9] The temperatures of the beginning of dissociation of the dimers are within 130−250 K.[3] Most probably, the dimerization temperature is defined by the initial distance between the $C_{60}^{\bullet-}$ radical anions and their environment from the countercations and solvent molecules.[3,7] Even in the same compound, the initial structural differentiation of the $C_{60}^{\bullet-}$ pairs, in which the dimerization is realized, can noticeably shift the dimerization temperatures.[7] The least-stable $(C_{60}^-)_2$ dimers were observed in $Cr(C_6H_6)_2{\cdot}C_{60}{\cdot}[Pd(dbdtc)_2]_{0.5}$.[9] Such dimerization is accompanied by a relatively large hysteresis between the cooling and heating curves (~20 K). As a result, at a fast cooling rate, the dimerization temperature decreases to 60 K.[9] The dimers with highest stability were found in $Cr(C_6H_5Me)_2{\cdot}C_{60}$, $Cr(C_6H_6)_2{\cdot}C_{60}{\cdot}C_6H_5CN$, and $Cp_2Co{\cdot}C_{60}{\cdot}C_6H_4Cl_2$.[5,6b] However, due to the fact that the dimers already begin to dissociate above 250 K, their observation is impossible at room temperature (RT). On the contrary, single-bonded $(C_{70}^-)_2$ dimers are essentially more stable and begin to dissociate only above RT. Due to that, their IR and vis−NIR spectra can be analyzed.[10] Recently, a negatively charged $(C_{60}^-)_2$ dimer bonded by two single bonds has been found in $\{Co^{II}TMPP{\cdot}(MDABCO^+)\}_2{\cdot}(C_{60}^-)_2{\cdot}(C_6H_4Cl_2)_{2.5}{\cdot}(C_6H_5CN)_{1.5}$ ($MDABCO^+$ = the cation of ***N***-methyldiazabicyclooctane; TMPP = tetrakis(4-methoxyphenyl)porphyrin).[11] This dimer differs in electronic state from the diamagnetic σ-$(C_{60}^-)_2$ dimer[3,6−8] and manifests approximately two spins per dimer at 300 K. Up to now, there has been only one example of the formation of such $(C_{60}^-)_2$ dimers, and the conditions, which define the formation of negatively charged $(C_{60}^-)_2$ dimers bonded by one or two single bonds in the ionic complexes, are not clear.

In this work, we present new ionic and neutral complexes of C_{60} with coordination $M^{II}TPP_2{\cdot}DMP$ assemblies (M = Mn (**1**) and Zn (**2**); TPP = tetraphenylporphyrin; DMP = *N*,*N*′-dimethylpiperazine). Their crystal structures and optical and magnetic properties were studied. It was shown that negatively charged σ-$(C_{60}^-)_2$ dimers formed in **1** have the highest stability among the ionic complexes of C_{60} studied to date. Moreover, the σ-$(C_{60}^-)_2$ dimers coexist in this complex with the $(C_{60}^-)_2$ dimers bonded by two single bonds. That allows one to understand the conditions, at which the formation of the $(C_{60}^-)_2$ dimers bonded by two single bonds is more preferable than that of the σ-$(C_{60}^-)_2$ dimers. The magnetic transition associated with the dissociation of the σ-$(C_{60}^-)_2$ dimers and their vis−IR spectra is discussed in detail. Molecular structures of new coordination $M^{II}TPP_2{\cdot}$DMP assemblies (M = Mn, Zn) are also presented for the first time.

Experimental Section

Materials. Zinc(II) tetraphenylporphyrin (ZnTPP), manganese(III) tetraphenylporphyrin chloride ($Mn^{III}TPPCl$), sodium borohydride ($NaBH_4$), diazabicyclooctane (DABCO), sodium ethanethiolate (CH_3CH_2SNa), *N*,*N*′-dimethylpiperazine (DMP), and methyl iodide (CH_3I) were purchased from Aldrich. $Mn^{II}TPP$ was obtained by the reduction of $Mn^{III}TPPCl$ by $NaBH_4$ in ethanol.[12] C_{60} of 99.98% purity was used from MTR, Ltd. The solvents were purified in an argon atmosphere. Chlorobenzene (C_6H_5Cl) and *o*-dichlorobenzene ($C_6H_4Cl_2$) were distilled over CaH_2 under reduced pressure, benzonitrile (C_6H_5CN) was distilled over Na under reduced pressure, and hexane was distilled over Na/benzophenone. The solvents were degassed and stored in a glovebox. All manipulations for the synthesis of air-sensitive **1** were carried out in a MBraun 150B-G glove box with a controlled atmosphere and the concentrations of H_2O and O_2 less than 1 ppm. The crystals were stored in a glovebox and sealed in 2 mm quartz tubes for electron paramagnetic resonance (EPR) and superconducting quantum interference device (SQUID) measurements under 10^{-5} Torr of pressure. KBr pellets for IR and UV−vis−NIR measurements were prepared in a glovebox.

Synthesis. *N*,*N*′-dimethyldiazabicyclooctane diiodide ($DMDABCO{\cdot}I_2$) was obtained by the dropwise addition of an excess of CH_3I (5 mL, 0.08 mol) to DABCO (2 g, 0.0178 mol) dissolved in 30 mL of acetonitrile at the stirring. After 2 h of stirring, a white crystalline precipitate of $DMDABCO{\cdot}I_2$ was formed. It was filtered off, washed with two portions of 10 mL of acetonitrile, and dried in a vacuum during a 8 h period. A mass of 4.94 g of $DMDABCO{\cdot}I_2$ was obtained with 70% yield. Elemental analysis (Calcd, I = 64.2%; Found, I = 63.8%).

The crystals of $\{(Mn^{II}TPP)_2{\cdot}DMP\}{\cdot}(C_{60})_2{\cdot}(DMETEP)_2{\cdot}(C_6H_4Cl_2)_5$ (**1**) (DMETEP = *N*,*N*′-dimethyl-*N*′-ethylthioethylpiperazine) were obtained by the following procedure. C_{60} (25 mg, 0.035 mmol), a 10-fold molar excess of CH_3CH_2SNa (30 mg, 0.36 mmol), and a 4-fold molar excess of $DMDABCO{\cdot}I_2$ (44.5 mg, 0.175 mmol) were stirred in 20 mL of the $C_6H_4Cl_2/C_6H_5CN$ (19:1) mixture for

(3) Konarev, D. V.; Khasanov, S. S.; Saito, G.; Lyubovskaya, R. N. *Recent Res. Devel. Chem*. **2004**, *2*, 105.

(4) (a) Zhu, Q.; Cox, D. E.; Fischer, J. E. *Phys. Rev. B: Condens. Matter Mater. Phys*. **1995**, *51*, 3966. (b) Oszlányi, G.; Bortel, G.; Faigel, G.; Tegze, M.; Grárásy, L.; Pekker, S.; Stephens, P. W.; Bendele, G.; Dinnebier, R.; Mihály, G.; Jánossy, A.; Chauvet, O.; Forró, L. *Phys. Rev. B: Condens. Matter Mater. Phys*. **1995**, *51*, 12228. (c) Kosaka, M.; Tanigaki, K.; Tanaka, T.; Atake, T.; Lappas, A.; Prassides, T. *Phys. Rev. B: Condens. Matter Mater. Phys*. **1995**, *51*, 12018.

(5) Hönnerscheid, A.; Wüllen, L.; Jansen, M.; Rahmer J.; Mehring, M. *J. Chem. Phys.* **2001**, *115*, 7161.

(6) (a) Konarev, D. V.; Khasanov, S. S.; Otsuka, A.; Saito, G. *J. Am. Chem. Soc*. **2002**, *124*, 8520. (b) Konarev, D. V.; Khasanov, S. S.; Saito, G.; Otsuka, A.; Yoshida, Y.; Lyubovskaya, R. N. *J. Am. Chem. Soc.* **2003**, *125*, 10074.

(7) Konarev, D. V.; Khasanov, S. S.; Kovalevsky, A. Y.; Saito, G.; Otsuka, A.; Lyubovskaya, R. N. *Dalton Trans.* **2006**, 3716.

(8) Ketkov, S. Yu.; Domrachev, G. A.; Ob'edkov, A. M.; Vasil'kov, A. Yu.; Yur'eva, L. P.; Mehner, C. P. *Russ. Chem. Bull*. **2004**, *53*, 1932.

(9) Konarev, D. V.; Kovalevsky, A. Y.; Otsuka, A.; Saito.; G.; Lyubovskaya, R. N. *Inorg. Chem*. **2005**, *44*, 9547.

(10) Konarev, D. V.; Khasanov, S. S.; Vorontsov, I. I.; Saito, G.; Antipin, Yu. A.; Otsuka, A.; Lyubovskaya, R. N. *Chem. Commun*. **2002**, 2548.

(11) Konarev, D. V.; Khasanov, S. S.; Otsuka, A.; Saito, G.; Lyubovskaya, R. N. *J. Am. Chem. Soc*. **2006**, *128*, 9292.

(12) (a) Wayland, B. B.; Olson, L. W.; Siddiqui, Z. U. *J. Am. Chem. Soc*. **1970**, *92*, 4235. (b) Kobayashi, H.; Yanagawa, Y. *Bull. Chem. Soc. Jpn*. **1972**, *45*, 450.

1 h at 60 °C. C_6H_5CN was added to increase the solubility of CH_3CH_2SNa and DMDABCO·I_2, which are poorly soluble in pure $C_6H_4Cl_2$. During stirring, the color of the solution changed from violet (characteristic of neutral C_{60}) to red-brown. After the cooling of the solution down to room temperature and filtering, the NIR spectrum was measured to indicate the selective reduction of C_{60} to the −1 charged state. $Mn^{II}TPP$ (24 mg, 0.035 mmol) was dissolved in the obtained solutions at 60 °C for 1 h, and the solution was cooled, filtered in a 50 mL glass tube of 1.8 cm diameter with a ground-glass plug, and 25 mL of hexane was layered over the solution. The diffusion was carried out during 2 months to give crystals of **1** on the wall of the tube. The solvent was decanted from the crystals, and they were washed with hexane (yield 50%). The crystals were black prisms with characteristic blue luster and up to 1 × 1 × 0.2 mm^3 in size. The composition of the complex was determined from X-ray structural analysis on a single crystal. Several crystals selected from the synthesis had similar unit-cell parameters.

The crystals of $\{(ZnTPP)_2\cdot DMP\}\cdot(C_{60})_2\cdot(C_6H_5Cl)_4$ (**2**) were obtained by the slow evaporation of chlorobenzene solution (15 mL) containing C_{60} (25 mg, 0.035 mmol), ZnTPP (23 mg, 0.035 mmol), and a large excess of DMP (1 mL). After 1 week, the crystals of **2** were formed, and they were washed with hexane (yield 70%). The crystals were rhomboids with characteristic blue luster and up to 2 × 1 × 0.4 mm^3 in size. The composition of **2** was determined from X-ray structural analysis.

General Procedures. UV−vis−NIR spectra were measured in KBr pellets on a Shimadzu-3100 spectrometer in the 240−2600 nm range. FT-IR spectra were measured in KBr pellets with a Perkin-Elmer 1000 Series spectrometer (400−7800 cm^{-1}). EPR spectra were recorded from 4 up to 360 K with a JEOL JES-TE 200 X-band ESR spectrometer equipped with a JEOL ES-CT470 cryostat. A Quantum Design MPMS-XL SQUID magnetometer was used to measure the static susceptibilities of polycrystalline **1** between 1.9 and 360 K at 100 mT static magnetic field. A sample-holder contribution and core-temperature-independent diamagnetic susceptibility (χ_0) were subtracted from the experimental values. The values of Θ and χ_0 were calculated using experimental data in the 40−300 K range with the appropriate formula: $\chi_M = C/(T - \Theta) + \chi_0$.

Crystal Structure Determination. X-ray diffraction data for **1** and **2** are listed in Table 1. The intensity data for the structural analysis of **1** were collected at 100(2) K on a MAC Science DIP-2020K oscillator type X-ray imaging plate diffractometer with graphite-monochromated Mo Kα radiation at low temperatures using an Oxford Cryostream cooling system. Raw data reduction to F^2 was carried out using the *DENZO* program.[13] X-ray diffraction data for **2** were collected at 100(2) using a Bruker Nonius X8 Apex diffractometer with CCD area detector (Mo Kα radiation, λ = 0.71073 Å) equipped with an Oxford Cryosystems nitrogen gas-flow apparatus. The data were collected by φ and ω-scans with 0.3° frame-width and 30 s exposure time per frame. The data were integrated, scaled, sorted, and averaged using the Bruker AXS software package.[14] The structures of **1** and **2** were solved by direct method and refined by the full-matrix least-squares method against F^2 using *SHELX-97*.[14] Non-hydrogen atoms were refined in the anisotropic approximation. Positions of hydrogen atoms were calculated geometrically. Subsequently, the positions of H atoms were refined by the "riding" model with $U_{iso} = 1.2U_{eq}$ of the connected non-hydrogen atom or as ideal CH_3 groups with $U_{iso} = 1.5U_{eq}$.

Table 1. X-ray Diffraction Data for **1** and **2**

	compound	
	1	**2**
structural formula	$\{(Mn^{II}TPP)_2\cdot DMP\}\cdot(C_{60})_2\cdot(DMETEP)_2\cdot(C_6H_4Cl_2)_5$	$\{(ZnTPP)_2\cdot DMP\}\cdot(C_{60})_2\cdot(C_6H_5Cl)_4$
empirical formula	$C_{264}H_{136}Cl_{10}Mn_2N_{14}S_2$	$C_{238}H_{90}Cl_4Zn_2N_{10}$
M_r (g·mol^{-1})	4032.37	3361.74
cryst color	black	black
size (mm × mm × mm)	0.5 × 0.5 × 0.2	0.4 × 0.3 × 0.2
cryst syst	triclinic	monoclinic
space group	$P\bar{1}$	$P2_1/n$
a (Å)	14.2060(5)	14.042(1)
b (Å)	15.2780(5)	30.700(2)
c (Å)	21.8810(7)	18.186(1)
α (deg)	90.668(2)	90
β (deg)	108.425(2)	105.794(2)
γ (deg)	94.286(2)	90
V (Å^3)	4489.9(3)	7545.8(8)
Z	1	2
ρ_{calc} (g/cm^3)	1.491	1.480
μ (mm^{-1})	0.385	0.462
F(000)	2070	3432
abs correction	empirical	multiscan
min/max transmission	0.91	0.93
T (K)	100(2)	100(2)
max 2Θ (deg)	54.8	56.70
reflns mesd	34 675	43 727
unique reflns	18 906	18 697
params, restraints	1698, 13 692	1708, 10 003
reflns [$F_o > 2\sigma F_o$]	16 912	12 800
R_1 [$F_o > 2\sigma F_o$]	0.0588	0.0597
wR_2 (all data)[a]	0.1632	0.1871
a	0.0858	0.1134
b	7.6043	0
GOF	1.019	1.087
restr GOF	0.982	0.901
CCDC nos	617720	617721

[a] $w = 1/[\sigma^2(F_o^2) + (aP)^2 + bP]$, $P = [\max(F_o^2, 0) + 2F_c^2]/3$.

Molecular Disordering in 1 and 2. The crystal structure of **1** contains ordered $DMETEP^+$ cations (Figure 1 d). One of the phenyl rings of $Mn^{II}TPP$ porphyrin in the $(Mn^{II}TPP)_2\cdot DMP$ units (Figure 1a) is disordered between two positions with the 85/15% occupancies. The position of the $(C_{60}^-)_2$ dimers is shared by the dimers of two types. The σ-$(C_{60}^-)_2$ dimer bonded by one single bond (Figure 1c) is disordered between two orientations with 73/13% occupancies (total occupancy is 86%). The $(C_{60}^-)_2$ dimer bonded by two single bonds has only 14% occupancy (Figure 1b). There are three positions of solvent $C_6H_4Cl_2$ molecules in **1**. These molecules are ordered in one position, whereas they are disordered between two orientations near the inversion center in the second position and between three orientations with the 84/9/7% occupancies in the third position. To calculate intermolecular distances and present the figures for **1** in the case of disordered units, we used only the major occupied orientation of the σ-$(C_{60}^-)_2$ dimer and one major occupied orientation of the phenyl rings of $Mn^{II}TPP$. In the crystal structure of **2**, the C_{60} molecules are disordered between three orientations with 34/33/33% occupancies. One of the phenyl rings of ZnTPP porphyrin in the $(ZnTPP)_2\cdot DMP$ unit is disordered between two positions with 71/29% occupancies. Solvent C_6H_5Cl molecules are ordered in one position, whereas they are disordered between four orientations with 39/22/20/19% occupancies in the second position. To calculate intermolecular distances and present the figures for **2** in the case of disordered units, we used only one 34% occupied orientation of the C_{60} molecules and one major occupied orientation of the phenyl rings of ZnTPP.

(13) (a) Otwinowski, Z. Minor, W. In *Processing of X-ray Diffraction Data Collection in Oscillation Mode*; Methods in Enzymology; Carter, C. W., Sweet, R. M., Eds.; Academic Press, 1997; p 276. (b) Sheldrick, G. M. *SHELX-97*; University of Göttingen: Göttingen, Germany, 1997.
(14) Bruker Analytical X-ray Systems; Madison, WI, 1999.

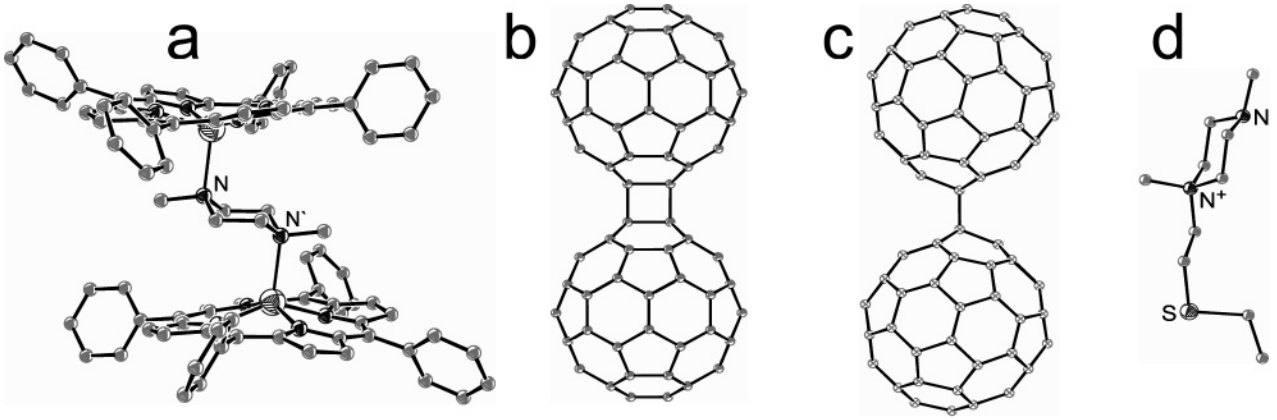

Figure 1. Molecular structures of the components of **1**: (a) (Mn^{II}TPP)·DMP assembly; (b) $(C_{60}^-)_2$ dimer bonded by two single bonds; (c) single-bonded $(C_{60}^-)_2$ dimer; and (d) *N*,*N*′-dimethyl-*N*′-ethylthioethylpiperazinium ($DMETEP^+$) cation.

Scheme 1

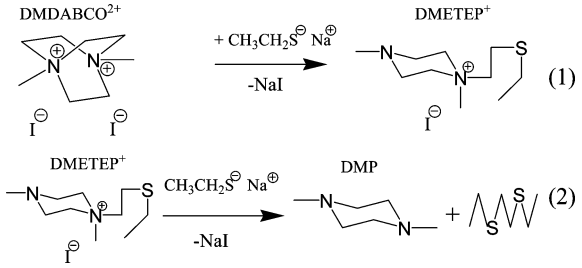

Results and Discussion

1. Synthesis. Complex **1** was obtained by the method developed for the synthesis of ionic multicomponent complexes containing metalloporphyrins, fullerene anions, and organic cations such as the cation of ***N***-methyldiazabicyclooctane: {M^{II}-porphyrin·$(MDABCO^+)_x$}·$(C_{60}^-)_x$·solvent (M = Co, Zn, Mn, Fe; x = 1 or 2).[11,15] In this work, we used another cation obtained by the reaction of an excess of CH_3I with DABCO. According to the elemental analysis, the obtained salt has the DMDABCO·I_2 composition and, therefore, contains $DMDABCO^{2+}$ dications. C_{60} was reduced by a large excess of CH_3CH_2SNa in the presence of an excess of DMDABCO·I_2. In contrast to previously used MDABCO·I, which was stable in the presence of CH_3CH_2SNa, DMDABCO·I_2 was found to be unstable. Most probably, the reaction is realized through a nucleophilic attack of $CH_3CH_2S^-$ to one of the positively charged nitrogen atoms of $DMDABCO^{2+}$; one $C-N^+$ bond is opened, one new C−S bond is formed, and the $DMDABCO^{2+}$ dication transforms to the $DMETEP^+$ cation (eq 1 of Scheme 1). Namely, $DMETEP^+$ cations were found in **1** and other complexes obtained by this method starting from DMDABCO·I_2. Moreover, most probably, the $DMETEP^+$ cations are also not so stable for the further nucleophilic attack of $CH_3CH_2S^-$ to the positively charged nitrogen atom of the $DMETEP^+$ cation, and one of the reaction products can be neutral DMP (*N*,*N*′-dimethylpiperazine) (eq 2 of Scheme 1). DMP forms coordination dimers with two Mn^{II}TPP units that allow the preparation of the ionic multicomponent complex {(Mn^{II}-TPP)$_2$·DMP}·$(C_{60}^-)_2$·$(DMETEP^+)_2$·$(C_6H_4Cl_2)_2$ (**1**), in which (C_{60}^-)·$(DMETEP^+)$ salt cocrystallizes with the neutral (Mn^{II}-TPP)$_2$·DMP units. The crystals of {$(ZnTPP)_2$·DMP}·C_{60}·C_6H_5Cl (**2**) were obtained by the slow evaporation of the chlorobenzene solution containing C_{60}, ZnTPP, and an excess of DMP.

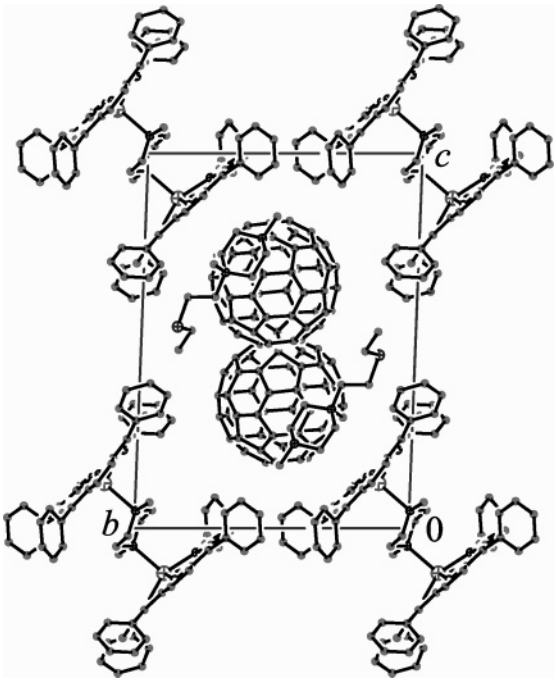

Figure 2. Projection of the crystal structure of **1** along the *a* axis and the zigzag chains formed by the alternating $(C_{60}^-)_2$ dimers and the $DMETEP^+$ cations.

2. Crystal Structures. The crystal structure of **1** was solved at 100(2) K. The main structural motif of **1** is the channels formed by four ($Mn^{II}TPP)_2$·DMP units (Figure 2), which are occupied by zigzag chains from the $(C_{60}^-)_2$ dimers alternating with the $DMETEP^+$ cations (the fragment of this chain is shown in Figure 3). These types of channels are characteristic of the ionic multicomponent complexes of metalloporphyrins with fullerene anions and were previously observed in (TMP^+)·{Co^{II}OEP·(C_{60}^-)}·$(C_6H_5CN)_x$·$(C_6H_4Cl_2)_{1-x}$ (TMP = tetramethylposphonium; OEP = octaethylporphyrin; $x \cong 0.75$) and {$(MDABCO^+)$·Co^{II}OEP·

(15) (a) Konarev, D. V.; Khasanov, S. S.; Otsuka, A.; Saito, G.; Lyubovskaya, R. N. *Chem.—Eur. J.* **2006**, *12*, 5225. (b) Konarev, D. V.; Khasanov, S. S.; Otsuka, A.; Saito, G.; Lyubovskaya. R. N. *Inorg. Chem.* **2007**, *46*, 2261.

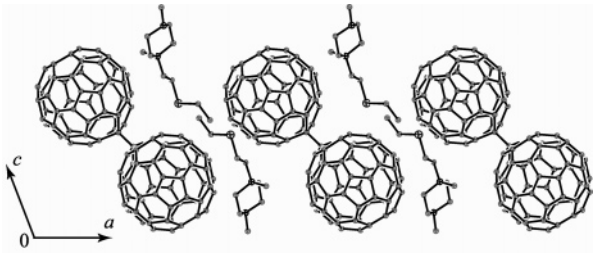

Figure 3. View of the zigzag chains of the alternating $(C_{60}^-)_2$ dimers and $DMETEP^+$ cations in the *ac* plane.

$(C_{60}^-)\}\cdot(C_6H_5CN)_x\cdot(C_6H_4Cl_2)_{1-x}$ ($x \cong 0.67$).[15a] However, in contrast to the $Co^{II}OEP$ complexes, in which the walls of the channels are built by the porphyrin planes of four Co^{II}-OEP units,[15a] the walls of the channels in **1** are built by two $Mn^{II}TPP$ porphyrin planes and phenyl substituents of two other $(Mn^{II}TPP)_2\cdot DMP$ units (Figure 2). The C_{60}^- anions are arranged in the chains in such a way that they are surrounded only by the phenyl substituents of the $(Mn^{II}TPP)_2\cdot DMP$ units with the van der Waals (vdW) C···C(C_{60}^-) and H···C(C_{60}^-) contacts in the 3.348−3.382 and 2.645−2.899 Å ranges. The $DMETEP^+$ cations are located exactly above the concave $Mn^{II}TPP$ porphyrin planes (rms is 0.156/0.203 Å).[16] In such a packing, there is no interaction between $Mn^{II}TPP$ porphyrin planes and C_{60}^- anions and the Mn···C(C_{60}^-) contacts are large (>6.9 Å).

The zigzag chains from the $(C_{60}^-)_2$ dimers pass along the *a* axis (Figure 3). The positions of the $(C_{60}^-)_2$ dimer are occupied by the major occupied σ-$(C_{60}^-)_2$ dimers (86% occupancy) and minor occupied $(C_{60}^-)_2$ dimers bonded by two single bonds (14% occupancy). The interfullerene center-to-center distance for the σ-$(C_{60}^-)_2$ dimer is 9.251 Å, and the length of a single interfullerene C−C bond is 1.587(4) Å (Figure 1c), as in other studied σ-$(C_{60}^-)_2$ dimers.[6−8] The $(C_{60}^-)_2$ dimer (Figure 1b) linked by two single bonds of 1.626(21) Å length has the interfullerene center-to-center distance of 9.054 Å (in previously described dimers of such type, these values were 1.581(3) and 9.070 Å).[11] In the chains, each σ-$(C_{60}^-)_2$ dimer forms two shortened vdW C−C contacts of 3.288 Å length by the 6-6 bonds with two neighboring σ-$(C_{60}^-)_2$ dimers (four such contacts are formed in total). The shortest interfullerene center-to-center distance between the C_{60}^- anions from the neighboring σ-$(C_{60}^-)_2$ dimers is 10.039 Å. The $DMETEP^+$ cations (Figure 1d) arrange in the zigzag chains of the C_{60}^- anions to form the vdW C···C(C_{60}^-) and H···C(C_{60}^-) contacts of 3.338 and 2.761−2.887 Å in length. The $C_6H_4Cl_2$ molecules mainly occupy cavities between the porphyrin planes in the $(Mn^{II}TPP)_2\cdot DMP$ units.

The molecular structure of the $(Mn^{II}TPP)_2\cdot DMP$ unit is shown in Figure 1a. This is a rare example of a coordination dimer of $Mn^{II}TPP$, whereas mainly coordination dimers and polymers containing $Mn^{III}TPP^+$ are described in the literature.[17] The formation of coordination dimers strongly deforms the $Mn^{II}TPP$ macrocycle to make Mn^{II} atoms five-coordinated. The averaged length of the Mn−N equatorial bonds in **1** is equal to 2.141(3) Å, and the displacement of the Mn^{II} atom from the porphyrin plane is 0.677 Å. Corresponding values for four-coordinated $Mn^{II}TPP$ are 2.084(2) and ∼0.177 Å,[18] and five-coordinated $Mn^{II}TPP\cdot MeIm$ units (MeIm = *N*-methylimidazole) are 2.128(2) and 0.57 Å.[19] The length of the axial Mn−N bond of 2.315(2) Å is noticeably longer in **1** than in the $Mn^{II}TPP\cdot MeIm$ units of 2.192(2) Å.[19] Therefore, the stronger distortion of the $Mn^{II}TPP$ macrocycle is attained in **1** at the longer axial Mn−N bond. The shortest distance between two Mn^{II} atoms bonded by the DMP ligand is 6.282 Å.

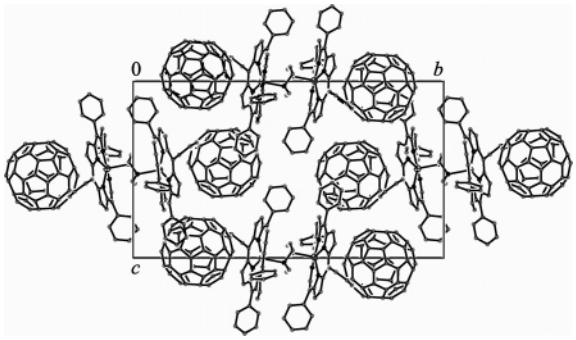

Figure 4. View of the crystal structure of **2** along the *a* axis.

The $(ZnTPP)_2\cdot DMP$ units form a neutral complex with fullerene, **2**. The crystal structure of **2** was studied at 100(2) K (Figure 4). The main building block of **2** is the C_{60}−$(ZnTPP)_2\cdot DMP$−C_{60} unit, in which each $(ZnTPP)_2\cdot DMP$ assembly forms vdW contacts with two C_{60} molecules arranged exactly above the concave ZnTPP macrocycle (rms is 0.188/0.207 Å,[16] Figure 4). The shortest Zn···C(C_{60}) distance of 3.235−3.268 Å and the vdW N···C(C_{60}) and C···C(C_{60}) contacts of 3.012−3.196 and 3.227−3.389 Å are typical for the C_{60} complexes with $(ZnTPP)_x\cdot L$ coordination units (x = 1, 2, and 4).[20a,b] The C_{60}−$(ZnTPP)_2\cdot DMP$−C_{60} units are arranged in such a way that zigzag chains from the C_{60} molecules can be outlined along the *c* axis. Each C_{60} molecule has two neighbors in the chain with the equal interfullerene center-to-center distance of 10.226 Å and only one vdW interfullerene C−C contact of 3.371 Å. The C_{60} chains are separated by the $(ZnTPP)_2\cdot DMP$ units along the *b* axis with the shortest interfullerene center-to-center distance of 14.183 Å and by the C_6H_5Cl molecules along the *a* axis with the shortest interfullerene center-to-center distance of 13.134 Å.

The molecular structure of the $(ZnTPP)_2\cdot DMP$ assembly is similar to that of the $(Mn^{II}TPP)_2\cdot DMP$ assembly (Figure 1a). The averaged lengths of the equatorial Zn···N bonds of 2.077(2) Å and the axial Zn−N(DMP) bond of 2.250(2) Å are noticeably shorter than the lengths of these bonds in the corresponding $(Mn^{II}TPP)_2\cdot DMP$ dimer. The displacement of

(16) Root-mean-square deviations (rms) were calculated for the porphyrin macrocycle excluding the metal atom (first value) and including the metal atom (second value).

(17) (a) Diskin-Posner, Y.; Kumar Patra, G.; Goldberg, I. *J. Chem. Soc., Dalton Trans.* **2001**, 2775. (b) Kumar, R. K.; Goldberg, I. *Angew. Chem., Int. Ed. Engl.* **1998**, *37*, 2027.

(18) Kirner, J. F.; Reed, C. A.; Scheidt, W. R. *J. Am. Chem. Soc.* **1977**, *99*, 1093.

(19) Kirner, J. F.; Reed, C. A.; Scheidt, W. R. *J. Am. Chem. Soc.* **1977**, *99*, 2557.

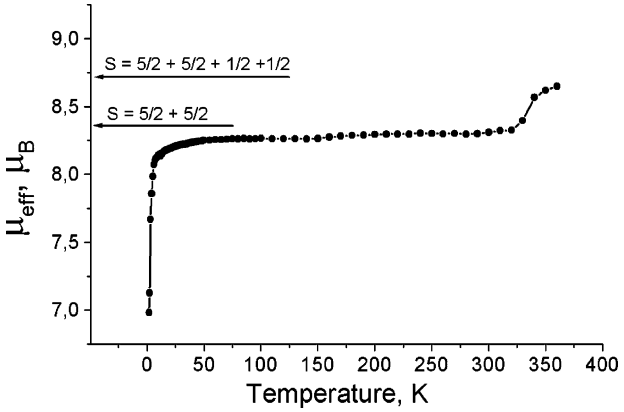

Figure 5. Temperature dependence of the magnetic moment of polycrystalline **1** in the 1.9−360 K range.

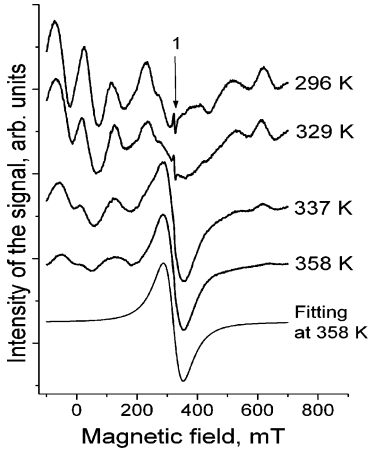

Figure 6. Changes in the EPR spectrum of polycrystalline **1** at the dissociation of the σ-$(C_{60}^-)_2$ dimers in the 320−360 K range.

Zn atom from the porphyrin plane is 0.485 Å. The shortest distance between two Zn atoms bonded by the DMP ligand is 6.263 Å. The geometric parameters of the five-coordinated ZnTPP·Py units in $(ZnTPP{\cdot}Py)_2{\cdot}C_{60}{\cdot}Cp_2Fe{\cdot}C_7H_8$ (Py = pyridine; Cp_2Fe = ferrocene)[20a] are close to those of the $(ZnTPP)_2$·DMP units in **2**. The averaged length of the equatorial Zn−N bonds is 2.072(2) Å, the length of the axial Zn−N(Py) bond is 2.151(4) Å, and the displacements of the Zn atom from the porphyrin plane is 0.435 Å.[20a]

3. Magnetic Properties of 1 and the Effect of the $(C_{60}^-)_2$ Dissociation on the Magnetic Properties. The magnetic moment of **1** at 300 K is equal to 8.33 μ_B per formula unit (Figure 5) and is close to the calculated value for two high-spin Mn^{II} centers ($S = {}^5/_2 + {}^5/_2$, $\mu_{eff} = 8.37\ \mu_B$). There is no contribution from the $C_{60}^{\bullet-}$ radical anions with $S = {}^1/_2$ spin state due to the dimerization. Therefore, σ-$(C_{60}^-)_2$ dimers are stable in **1** even at 300 K. Such high stability has for the first time been observed for the σ-$(C_{60}^-)_2$ dimers. Previously, the highest temperature for the beginning of dissociation of the dimers was found to be 250 K.[5,6a] The contribution from the paramagnetic $(C_{60}^-)_2$ dimers bonded by two single bonds to magnetic susceptibility should be small as that compared with high-spin Mn^{II} due to the small occupancy factors for these dimers. The magnetic moment is nearly constant down to 40 K, below which it begins to decrease due to antiferromagnetic interaction of spins. The magnetic susceptibility follows the Curie−Weiss law in the 300−40 K range with the Weiss constant of −0.5 K. The absence of noticeable magnetic interactions is associated with the formation of the diamagnetic σ-$(C_{60}^-)_2$ dimers, which magnetically dilute the paramagnetic species in **1**. The shortest distance between the Mn^{II} centers is in the $(Mn^{II}TPP)_2$·DMP dimer and most probably weak antiferromagnetic exchange interaction between the Mn^{II} centers is realized through the DMP ligand.

Complex **1** demonstrates an unusual EPR spectrum at RT, which it qualitatively retains down to 4 K. The features of the spectrum spread almost over the full range of electromagnetivity (0−0.7 T) with the separation between the components from 90 to 130 mT (Figure 6). Since the σ-$(C_{60}^-)_2$ dimers are EPR silent and the contribution of $(C_{60}^-)_2$ dimers bonded by two single bonds is negligible, the signal can be attributed mainly to the $(Mn^{II}TPP)_2$·DMP units. Generally, four-coordinated Mn^{II}TPP, five-coordinated Mn^{II}TPP·(*N*-MeIm), and six-coordinated $Mn^{II}TPP{\cdot}(MDABCO^+)_2$ units manifest asymmetric signals with $g_\perp \cong 6.0$ and $g \cong 2.0$ and hyperfine splitting from ^{55}Mn.[21,15b] The appearance of a different spectrum in **1** can be explained by zero-field splitting (ZFS) due to a strongly distorted environment of the Mn^{II} centers[22] or noticeable magnetic-exchange interaction between two Mn^{II} centers in the $(Mn^{II}TPP)_2$·DMP units. In the latter case, the spectrum of **1** can be more characteristic of the binuclear Mn^{II} complexes.[23] Indeed, a similar EPR spectrum with the features spread over the 0−0.5 T range was shown by manganese(II) diethyldithiocarbamate dimers, $\{Mn(Et_2\text{-}dtc)_2\}_2$, in the complex with C_{70}[23a] and binuclear manganese(II) complexes bridged, for example, by chlorine atoms.[23c]

The magnetic moment of **1** begins to increase above 320−330 K (Figure 5) up to 8.66 μ_B at 360 K. This value is close to that calculated for the system of four noninteracting spins ($S = {}^5/_2 + {}^5/_2 + {}^1/_2 + {}^1/_2$, $\mu_{eff} = 8.72\ \mu_B$). Therefore, at 360 K most parts of the diamagnetic σ-$(C_{60}^-)_2$ dimers dissociate to paramagnetic $C_{60}^{\bullet-}$ radical anions. The EPR spectrum of **1** also strongly changes above 330 K. An EPR signal attributed to the $(Mn^{II}TPP)_2$·DMP units decreases in intensity with the temperature increase, and a new broad Lorenz signal with $g = 2.0179$ and $\Delta H = 65.5$ mT grows (Figure 6). The temperatures for the increase of the magnetic moment and

(20) (a) Konarev, D. V.; Kovalevsky, A. Y.; Li, X.; Neretin, I. S.; Litvinov, A. L.; Drichko, N. V.; Slovokhotov, Y. L.; Coppens, P.; Lyubovskaya, R. N. *Inorg. Chem.* **2002**, *41*, 3638. (b) Litvinov, A. L.; Konarev, D. V.; Kovalevsky, A. Y.; Coppens, P.; Lyubovskaya, R. N. *Cryst. Growth Des.* **2005**, *5*, 1807. (c) Hosseini, A.; Taylor, S.; Accorsi, G.; Armaroli, N.; Reed, C. A.; Boyd, P. D. W. *J. Am. Chem. Soc.* **2006**, *128*, 15903.

(21) Reed, C. A.; Kouba, J. K.; Grimes, C. J.; Cheung, S. K. *Inorg. Chem.* **1978**, *17*, 2666.

(22) Goodgame, D. M. L.; El Mkami, H.; Smith, G. M.; Zhao, J. P.; McInnes, E. J. L. *Dalton Trans.* **2003**, 34.

(23) (a) Konarev, D. V.; Kovalevsky, A. Y.; Khasanov, S. S.; Saito, G.; Lopatin, D. V.; Umrikhin, A. V.; Otsuka, A.; Lyubovskaya, R. N. *Eur. J. Inorg. Chem.* **2006**, 1881. (b) Khangulov, S. V.; Pessiki, P. J.; Barynin, V. V.; Ash, D. E.; Dismukes, G. C. *Biochemistry* **1995**, *34*, 2015. (c) Romero, I.; Collomb, M.-N.; Deronyier, A.; Llobet, A.; Perret, E.; Pèkaut, J.; Le Pare, L.; Latour, J.-M. *Eur. J. Inorg. Chem.* **2001**, 69.

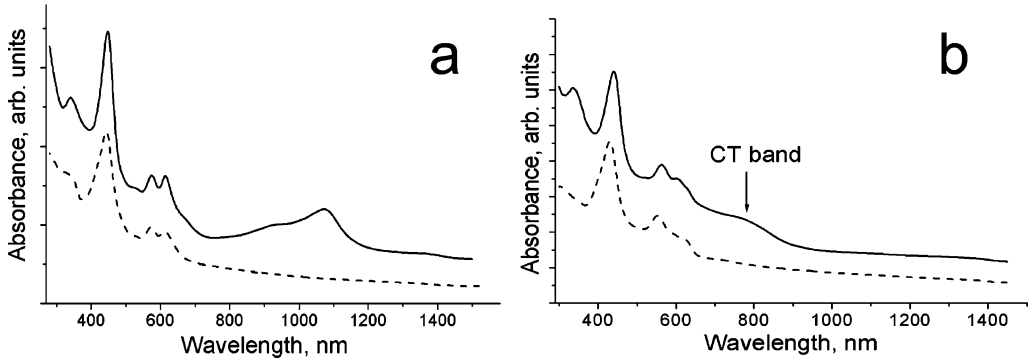

Figure 7. UV−vis−NIR spectra of **1** (a) and **2** (b). The spectra of starting $Mn^{II}TPP$ (a) and ZnTPP (b) are shown below by dashed lines.

the appearance of a new signal coincide. Therefore, the changes in the EPR spectrum can be unambiguously attributed to the formation of the EPR-active $C_{60}^{\bullet-}$ radical anions. Most probably, the new signal appears due to exchange coupling between paramagnetic $(Mn^{II}TPP)_2$·DMP and $C_{60}^{\bullet-}$ species, and it should have a *g*-factor value intermediate between those characteristic of the $(Mn^{II}TPP)_2$·DMP and $C_{60}^{\bullet-}$ species (1.9996−2.0000).[24] As a rule, exchange interaction leads to the disappearance of any individual features of the signals (such as ZFS splitting and the asymmetry of the signal) and provides the pure Lorenz shape of the resulting single line. The changes in the EPR spectra were always observed at the dissociation of the σ-$(C_{60}^{-})_2$ dimers. Asymmetric EPR signals characteristic of individual cations in the dimeric phase are transformed in the monomeric phase to the Lorenz signals, with g-factor values intermediate between those characteristic of the cations and the $C_{60}^{\bullet-}$ species.[3,6a,7,9]

The $(C_{60}^{-})_2$ dimers bonded by two single bonds show the EPR signal.[11] On the background of a very intense EPR signal from Mn^{II}, the EPR spectrum of these dimers is not resolved, probably due to a small content of the dimers as well as the fact these dimers can give one signal together with some part of the $(Mn^{II}TPP)_2$·DMP units due to exchange coupling between them. There is only one weak signal with $g = 1.9915$ and $\Delta H = 4.98$ mT at RT that can be attributed to negatively charged fullerene species (Figure 6, arrow 1). However, most probably it arises from a small fraction (≤1%) of nondimerized $C_{60}^{\bullet-}$radical anions, which were previously observed in the dimeric phases of ionic fullerene complexes (up to 3.5% from total amount of C_{60} molecules).[6b] This signal strongly narrows with the temperature decrease and shows a paramagnetic dependence of intensity at low temperatures.

4. IR and UV−vis−NIR Spectra. Since the IR spectrum of the $DMETEP^+$ cations is unknown, the analysis of the spectrum of **1** is hampered. Nevertheless, in addition to the absorption bands characteristic of the $Mn^{II}TPP$, DMP, and solvent molecules, there are many additional absorption bands (Supporting Information), which should be not only from the $DMETEP^+$ cations but also due to the fact that dimerization breaks the symmetry in C_{60} and manifests IR silent modes. Similarly, additional weak absorption bands are observed in the spectrum of the $(C_{60}^{-})_2$ dimers bonded by two single bonds.[11] The spectrum of **2** is simpler and indicates the neutral ground state of the complex (Supporting Information). The $F_{1u}(4)$ mode of C_{60} is split into three bands centered at 1419, 1424, and 1428 cm^{-1}. Such splitting justifies the freezing of the C_{60} molecules' rotation, even at RT.[25]

The UV−vis−NIR spectrum of **1** in KBr pellet shows characteristic bands of $Mn^{II}TPP$ at 448, 575, and 614 nm and negatively charged C_{60} at 342, 954, 1073, and 1356 nm (Figure 7a). The bands of $Mn^{II}TPP$ (443, 572, and 611 nm) remain unchanged qualitatively and are shifted only by 3−5 nm at the formation of the $(Mn^{II}TPP)_2$·DMP units. However, parent $Mn^{II}TPP$ can contain coordinated ethanol since it was obtained in ethanol.[21] In this case, the Soret band of starting $Mn^{II}TPP$ is additionally shifted to the red side and the real shift of the Soret band at the formation of **1** can be larger than 5 nm. Previously, it was shown that the Soret band at 434 nm in the spectrum of $Mn^{II}TPP$·$(C_6H_5Me)_2$ in THF was shifted to 440 nm in the spectrum of $Mn^{II}TPP$·(*N*-MeIm)·$(THF)_{0.8}$.[21]

The UV−vis−NIR spectrum of **2** in KBr pellet manifests bands of ZnTPP at 440, 562, and 600 nm and a broad intense band with the maximum at 780 nm, which can be ascribed to charge transfer from the $(Zn^{II}TPP)_2$·DMP units to C_{60} (Figure 7b). The appearance of this band is associated with a relatively good overlapping of the π orbitals of concave ZnTPP porphyrin macrocycles and spherical C_{60} molecules.[20b,c] Starting ZnTPP has the bands at 431, 553, and 623 nm. Therefore, at the formation of the coordination dimers in **2**, the Soret band is noticeably shifted up to 9 nm, and the positions and relative intensities of the Q bands are changed. Similar charge-transfer bands with close positions of the maxima at 760−820 nm and the shifts of the Soret and Q bands of ZnTPP were observed at the formation of other C_{60} complexes with the $(ZnTPP)_x$·L coordination units (x = 1, 2, and 4).[20b] The absence of the absorption bands of $C_{60}^{\bullet-}$ in the NIR spectrum of **2** indicates the neutral ground state of the complex.

5. Comparison of the Optical Spectra of Negatively Charged $(C_{60}^{-})_2$ Dimers and $C_{60}^{\bullet-}$. The vis−NIR spectrum of the σ-$(C_{60}^{-})_2$ dimers in **1** was compared with those of the

(24) Reed, C. A.; Bolskar, R. D. *Chem. Rev.* **2000**, *100*, 1075.

(25) Semkin, V. N.; Drichko, N. V.; Kimzerov, Yu, A.; Konarev, D. V.; Lyubovskaya, R. N.; Graja, A. *Chem. Phys. Lett.* **1998**, *295*, 266.

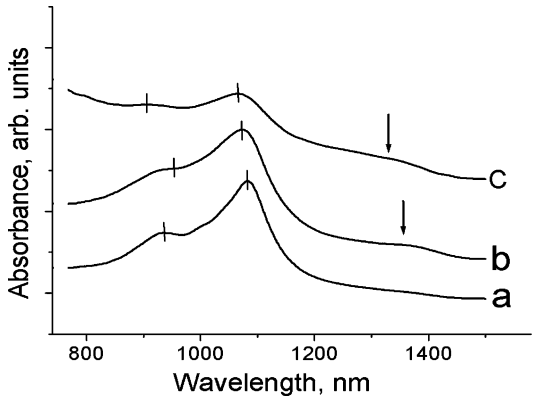

Figure 8. NIR spectra of (a) monomeric $C_{60}^{\bullet-}$ radical anions in $\{Mn^{II}TPP\cdot(MDABCO^{+})_2\}\cdot(C_{60}^{\bullet-})_2\cdot(C_6H_4Cl_2)_{4.2}\cdot(C_6H_5CN)_{1.8}$;[15b] (b) single-bonded σ-$(C_{60}^{-})_2$ dimer in **1**; and (c) $(C_{60}^{-})_2$ dimer bonded by two single bonds in $\{Co^{II}TMPP\cdot(MDABCO^{+})\}_2\cdot(C_{60}^{-})_2\cdot(C_6H_4Cl_2)_{2.5}\cdot(C_6H_5CN)_{1.5}$.[11]

$(C_{60}^{-})_2$ dimer bonded by two single bonds and monomeric $C_{60}^{\bullet-}$ radical anions (Figure 8). The $(C_{60}^{-})_2$ dimers bonded by two single bonds are probably admixed to the σ-$(C_{60}^{-})_2$ dimers in **1** at RT. However, the content of this dimer is too low to qualitatively change the spectrum. The $C_{60}^{\bullet-}$ radical anions have characteristic bands in the NIR range at 1083 and 937 nm, which allow an unambiguous identification of the -1 charged state of C_{60} in ionic complexes. Two similar bands are observed in the NIR spectra of the fullerene dimers with the shifts of both bands to 954 (17 nm) and 1072 nm (11 nm) for the dimer bonded by one single bond and 905 (32 nm) and 1064 nm (19 nm) for the dimer bonded by two single bonds. Noticeable broadening of both bands is also observed in comparison with the bands of monomeric $C_{60}^{\bullet-}$ (Figure 8). The NIR spectra of the dimers are different from that of $C_{60}^{\bullet-}$ by the appearance of weak additional low-energy bands at 1356 nm (the σ-$(C_{60}^{-})_2$ dimers) and 1330 nm (the $(C_{60}^{-})_2$ dimer bonded by two single bonds). Most probably these bands are associated with charge transfer between two C_{60}^{-} anions in the dimer. The appearance of additional bands in the NIR range accompanies the formation of all σ-bonded structures with negatively charged fullerenes. For example, the σ-bonded ($Co^{II}TPP\cdot C_{60}^{-}$) anions manifest bands at 1092 and 1288 nm;[26] ($Co^{II}TPP\cdot C_{60}(CN)_2^{-}$) anions at 1071 and ~1210 nm;[26a] and σ-bonded ($Co^{II}OEP\cdot C_{60}^{-}$) anions at 1086 and 1277 nm.[15a] The position of the first band is close to that of the band of the intramolecular transitions in the corresponding fullerene anions, whereas the broad low-energy bands can also be attributed to charge transfer between the fullerene anion and Co^{II}porphyrin in the σ-bonded units. The attribution is more complicated for the single-bonded $(C_{70}^{-})_2$ dimer showing two bands at 880 and 1240 nm.[10,6a] Since nonbonded $C_{70}^{\bullet-}$ radical anions manifest one band at 1363−1386 nm,[24] which correspondingly shifts at the dimerization, it is difficult to correctly assign the bands of the $(C_{70}^{-})_2$ dimer in the NIR range at present.

The spectral features of the negatively charged $(C_{60}^{-})_2$ dimers are similar to those observed for the electrochemically reduced forms of $C_{120}O$ and $C_{120}OS$ dimers in solution.[27] They manifest NIR bands at 940 and 1020 nm, respectively, which are also essentially broadened in comparison with these bands of monomeric $C_{60}^{\bullet-}$. So, this broadening can reflect the derivative nature of the dimers. Both reduced $C_{120}O$ and $C_{120}OS$ dimers also display additional broad low-energy bands associated with the intradimer CT transitions.[27]

Conclusion

In this work, we showed that coordination assemblies of metal tetraphenylporphyrins, $(M^{II}TPP)_2\cdot DMP$ (M = Mn, Zn; DMP = *N*,*N*′-dimethylpiperazine) can be successfully used as building blocks for the preparation of ionic multicomponent and neutral complexes with fullerenes (**1** and **2)**. The effective packing of the coordination assemblies with the C_{60} anions and molecules is promoted by the presence of flexible phenyl substituents in the $Mn^{II}TPP_2\cdot DMP$ units (**1**) and the concave shape of the ZnTPP macrocycles in the $ZnTPP_2\cdot DMP$ units (**2**). The $C_{60}^{\bullet-}$ radical anions are dimerized in **1** to form two types of dimers: major occupied single-bonded $(C_{60}^{-})_2$ dimer and minor occupied $(C_{60}^{-})_2$ dimer bonded by two single bonds. This is the first example of an ionic complex in which both types of negatively charged $(C_{60}^{-})_2$ dimers are formed. The diamagnetic single-bonded σ-$(C_{60}^{-})_2$ dimers begin to dissociate in **1** only above 320−330 K. These dimers have the highest stability among all σ-$(C_{60}^{-})_2$ dimers studied to date. The dissociation of the $(C_{60}^{-})_2$ dimers noticeably expands the space occupied by two C_{60}^{-} anions and rearranges all components of the complex. As a result, the environment formed by donors, countercations and solvent molecules and the mutual vdW and ionic bonding between them affects dimer stability and their dissociation temperatures. This effect can be compared with "pressure", which stabilizes the dimers, preventing their dissociation. Most probably this pressure is the highest in **1** as compared with other ionic complexes, in which σ-$(C_{60}^{-})_2$ dimers are formed. In this context, the appearance of the $(C_{60}^{-})_2$ dimers bonded by two single bonds in **1** is expected. The interfullerene center-to-center distance of 9.054 Å in these dimers is noticeably shorter than the distance of 9.251 Å in σ-$(C_{60}^{-})_2$ dimers. In this case the pressure should stabilize the more compact $(C_{60}^{-})_2$ dimers bonded by two single bonds rather than σ-$(C_{60}^{-})_2$ dimers, increasing their relative content. In the limiting case, a pure phase with the $(C_{60}^{-})_2$ dimers bonded by two single bonds is formed, as in $\{Co^{II}TMPP\cdot(MDABCO^{+})\}_2\cdot(C_{60}^{-})_2\cdot(C_6H_4Cl_2)_{2.5}\cdot(C_6H_5CN)_{1.5}$, in which the dimers are located in the porphyrin cell held together by the vdW forces.[11]

The dissociation of the single-bonded $(C_{60}^{-})_2$ dimers above 320−330 K results in the increase of the magnetic moment of **1** in accordance with the formation of two new $^1/_2$ spins from $C_{60}^{\bullet-}$. The EPR signal of the dimeric phase was attributed to the $(Mn^{II}TPP)_2\cdot DMP$ units. The dissociation of the σ-$(C_{60}^{-})_2$ dimers manifests a new broad Lorenz signal with $g = 2.0179$ and $\Delta H = 65.5$ mT, which most probably

(26) (a) Konarev, D. V.; Khasanov, S. S.; Otsuka, A.; Yoshida, Y.; Saito, G. *J. Am. Chem. Soc*. **2002**, *124*, 7648. (b) Konarev, D. V.; Khasanov, S. S.; Otsuka, A.; Yoshida, Y.; Lyubovskaya, R. N.; Saito, G. *Chem.—Eur. J*. **2003**, *9*, 3837.

(27) Dunsch, L.; Rapta, P.; Gromov, A.; Staško, A. *J. Electroanal. Chem*. **2003**, *547*, 35.

appears due to exchange coupling between paramagnetic $(Mn^{II}TPP)_2$·DMP and $C_{60}^{\bullet-}$ species.

The vis−NIR spectrum of the σ-$(C_{60}^{-})_2$ dimers shows bands similar to those observed in the spectrum of $C_{60}^{\bullet-}$ (with a shift of 11−17 nm) and a new band at 1356 nm, which can be attributed to charge transfer between two C_{60}^{-} anions in the dimer. Similar additional low-energy bands were observed in the spectra of the $(C_{60}^{-})_2$ dimer bonded by two single bonds[11] and σ-bonded units formed by Co^{II}porphyrins and C_{60}^{-} anions.[15a,26b]

Molecular structures of the coordination $(M^{II}TPP)_2$·DMP assemblies (M = Mn, Zn) were studied for the first time. Their formation elongates the equatorial M−N(DMP) bonds and displaces the M^{II} atom from the porphyrin plane toward the ligand. Such changes are greater at the formation of the $(Mn^{II}TPP)_2$·DMP units in **1** as compared with the $(ZnTPP)_2$·DMP units in **2** and five-coordinated Mn^{II}TPP·MeIm units.[19] The data obtained show that the bidentant DMP ligand can be used in the design of new coordination assemblies with metalloporphyrins.

Acknowledgment. The work was partly supported by Grant-in-Aid Scientific Research from the Ministry of Education, Culture, Sports, Science and Technology, Japan (152005019, COE programs) and the Russian Science Support Foundation, INTAS YSF 05-109-4653 and RFBR Grant N 06-03-32824 and RFBR-JSPS grant N 06-03-91361.

Supporting Information Available: Crystallographic data for **1** and **2** in CIF format; IR spectra data for starting compounds and **1** and **2** (Tables S1 and S2); geometry of TPP macrocycles (selected bond distances and bond angles in M^{II}TPP (M = Mn, Zn); and shortest metal−ligand (M···N), porphyrin−fullerene, and fullerene−fullerene contacts (Table S3). This material is available via the Internet at http://pubs.acs.org

IC061628Z